International Journal of Engineering Research and Applications (IJERA) ISSN: 2248-9622
NATIONAL CONFERENCE on Developments, Advances & Trends in Engineering Sciences
(NCDATES- 09th & 10th January 2015)

RESEARCH ARTICLE OPEN ACCESS

Applications of Artificial Neural Network for Condition Monitoring of Rolling Element Bearings

Vinay. M.S[1], H K Srinivas[2]
[1](Student, PG, Department of Mechanical Engineering, HITS, RR Dist, Telangana, India)
[2] (Prof& Head, Department of Mechanical Engineering, YDIT, Bangalore, Karnataka, India)

ABSTRACT
The vibration analysis of rotating machinery indicates the condition of potential faults such as unbalance, bent shaft, shaft crack, bearing clearance, rotor rub, misalignment, looseness, oil whirl & whip and other malfunctions. More than one fault can occur in a rotor & bearing. This paper describes the application of Artificial Neural Network (ANN) and Condition monitoring. Diagnosis involves intermittent or continuous collection and interpretation of data relating to the condition of critical components. Constant monitoring of machinery has been considered to be an essential and integral part of any modern rotating machinery facility, because any unexpected failure or breakdown will result in costly consequences. Adequate monitoring greatly reduces the frequency of breakdowns before they actually occur. The present study aims at developing a method of bearing condition estimation using neural networks which give higher success rates in their condition estimation than the existing methods. A multi-layered feed forward neural network trained with Error Back Propagation (EBP) algorithm has been used. This neural network has an edge over conventional monitoring method that can classify the condition of machine components even in the absence of explicit input–output relationships. Besides, the network can classify well even in the case of noisy or incomplete information obtained from the signals being monitored.

Keywords: Artificial Neural Networks, Rotor faults, Rotor test rig, Unbalance and bearing clearance, Vibration analysis and Wavelet.

I. INTRODUCTION

Determining the health and status of the machine is of prime importance in maintenance and condition monitoring is one of the most efficient and reliable method. Condition monitoring implies determining the condition of a machine or a device and the pace and nature of its change with time. The condition of the machine may be determined by analysing the physical parameters viz. vibration, noise, temperature, oil contamination, wear debris etc. A change in any of these parameters is called signature and indicates a change in condition or health of the machine.With the recent developments in the field of microprocessors, signal processing and signal conditioning technology happening; it allows the development of powerful, efficient, and very cost effective systems for ontinuous condition monitoring of different machine parameters. Reasons that made the condition monitoring of machinery a necessity are

- EliminatingUnnecessary Disassembly
- Reducing Unscheduled Downtime
- Avoiding Wrecks
- Economic Consideration

1.1 TYPES OF CONDITION MONITORING

There are several types of condition monitoring techniques. Table 1shows the different conditioning monitoring techniques, used for various applications, which can be used for machine fault diagnosis. Some of them are explained here.

A. Wear Debris Monitoring
B. Performance/ Behaviour Monitoring
C. Temperature Monitoring
D. Vibration Monitoring

II. ARTIFICIAL NEURAL NETWORKS

The neural network techniques are used in conjunction with signal analysis techniques for classification and quantification of faults [8]. Kaminski [9] has developed neural networks to identify the approximate location of damage. McCormick and Nandi [10] have used neural network method for automatically classifying the machine condition using vibration time series. Vyas and Satish Kumar [11] have carried out studies to generate data for rotating machinery faults. Srinivasan [12] also carried out studies on faults (parallel misalignment, angular misalignment, bearing clearanceetc). The Fig 2.1 shows a simple network consisting of three layers with one input layer, one hidden layer and one output layer. There

are no connections between nodes in the same layer and no connection that bridge the layers. Such networks with only one hidden layer can uniformly approximate any continuous function and therefore provide a theoretical basis for the use of this type of network. The input-output relationship of each node is determined by a set of connection weights W_i, a threshold parameter bi and a node activation function A (.) such that-

$$Y = A\,(Wi\ Xi + bi) \quad (1)$$

Where Y is the output of the node and Xi are the inputs. The activation function A (.) defines the output of a neuron in terms of activity level at its input. The sigmoid function is the most common activation function used in neural networks. It is defined as a strictly increasing function that exhibits smoothness and asymptotic properties. The Tan-sigmoid activation function is used in the hidden layer. The purelin activation function is used in the output layer.

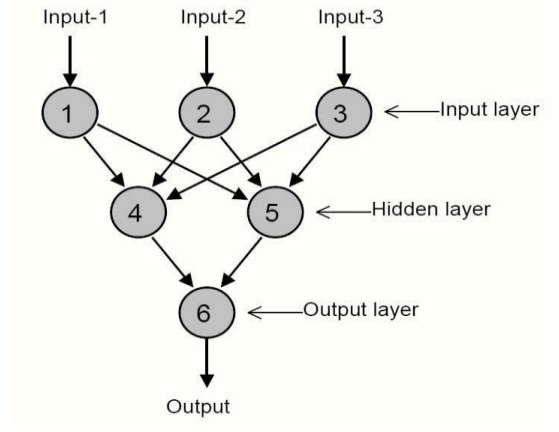

Fig 2.1 Three- layers network

In the present work, improved back propagation neural network has been applied for the diagnosis of combined faults of unbalance and bearing clearance. It attempts to minimize the square of the error between the output of the network and the desired outputs by changing the connection weights that use some form of gradient descent. The back propagation method has used gradient descent techniques, which are simply the techniques, where parameters such as weights and biases are moved in the opposite direction towards the error gradient. The Levenberg-Marquardt algorithm has the best convergence speeds for small and medium size networks [13, 14]. This optimization technique is more accurate and faster than gradient descent method. The Levenberg-Marquardt update rule is-

$$\Delta W = (J^T J + \Delta\mu\ I)\ J\ Te \quad (2)$$

Where ΔW = Small change in weight. J is the n by m Jacobian matrix $J^T J$ to keep function N rows of J linearly independent and μ is a small positive constant chosen to ensure ($J^T J$+ μI) is positive for all „n" values. If μ is very large the above expression approximates gradient descent; if it is small, the above expression becomes the Gauss-Newton method. The Gauss-Newton method is faster, more accurate and near to an error minimum. Training continues until the error goal is met, the minimum error gradient occurs, the maximum value of μ occurs, or the maximum number of epochs has been finished. The MAT LAB Neural Network toolbox has been applied for diagnosing the rotating machinery faults.

III. EXPERIMENTATION

3.1 NECESSARY INSTRUMENTATION

The instruments used in bearing condition monitoring are, a transducer to convert the vibration signals into the electrical signals and the frequency analyser to convert the time domain signals into the frequency domain.

3.2 TRANSDUCER

For vibration data, acquisition three main types of the transducers can be used viz. displacement probes, velocity transducers, and accelerometers

The piezoelectric accelerometer is used as a transducer in this experimental work to collect the vibration data. The piezoelectric crystal in the accelerometer converts mechanical energy into electrical signals. Data acquired with this type of transducer are relative acceleration expressed in terms of the gravitational constant g. This general-purpose accelerometers have effective range of about 1 to 10 kHz. Hence the accelerometer is used in bearing condition monitoring. Also the accelerometers does not require calibration program. However, these are

.	**Vibration Analysis**	**Noise Analysis**	**Acoustic Emission**	**Debris Analysis**	**Thermal Imaging**	**Corrosion Monitoring**
Bearing	YES	YES	YES	YES	YES	YES
Boiler			YES		YES	
Compressor	YES	YES		YES	YES	
Coupling	YES	YES				
Elevators	YES	YES			YES	YES
Excavators	YES				YES	YES
Filters				YES		YES
Gearboxes	YES	YES	YES	YES	YES	YES
M/c Tools	YES	YES				
Pr. Vessels			YES		YES	YES
Pumps	YES	YES			YES	YES
Structures	YES		YES			YES
Transformers					YES	
Turbines	YES	YES	YES	YES	YES	YES
Welding			YES			
I.C. Engine					YES	YES

table 1: Shows the different conditioning monitoring techniques, used for various applications.

susceptible to high temperature, which may damage the piezoelectric crystal.

3.3 FAST FOURIER TRANSFORM ANALYZER

It is an electronic device that is capable of taking the time waveform of a given signal and converting it into its frequency domain component.

3.4 MATHEMATICAL BACKGROUND

Baron Jean Baptiste Fourier showed that any wave can be generated by adding up sine waves of the integral multiples of the frequency 'ω'. In other words, any wave can be split into a series of harmonic functions, the frequency of which is the integral multiples of the frequency 'ω'as shown in figure 3.1.

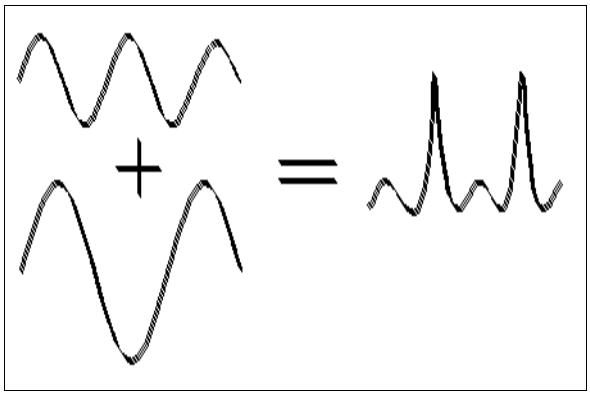

Fig 3.1 Components of real waveform

Mathematically it can be written as ∞

$$f(t) = a_0 + \Sigma (a_n \cos n\omega t + b_n \sin n\omega t) \quad \ldots\ldots(1)$$
$$n=1$$

Where
F(t) : Periodic function
a0 : Constant.
ω: Harmonic Frequency
a1, a2, a3 …. an& b1 ,b2 ,b3….bn : Amplitudes of individual sine waves

The series given by equation (1) is called Fourier series. The harmonic frequency ω is called the fundamental or the first harmonic of the f(t) and harmonic frequency nω is called the nth harmonic. The splitting up of harmonic function into series of harmonic functions is called harmonic analysis. [10]

3.5 WORKING OF FFT ANALYZER

The properly selected accelerometer should be used to provide an electrical signal proportional to acceleration to the input jack of FFT analyser. The processing of this signal into a valid frequency spectrum involves followingsteps.

- **Signal conditioning:** It is always recommended that the full voltage range of the A/D converter is used. Hence, before a signal is input to the A/D converter, it is conditioned or scaled (figure 3.2).Conversely, it is important not to under drive the converter. Assuming an A/D converter has a full voltage range of +/- 10 volts, then without pre-scaling, a small, 1 volt input signal would not be digitally converted with the available resolution effectively utilizing fewer bits than that available and hence would suffer a poorer signal to noise ratio.It is equally important to ensure that the voltage range of the input signal is not greater than that of the A/D converter. If it is greater than A/D converter voltage then the signals above the converter voltage are lost and it is called clipping. Any signal, which falls outside the upper and lower voltage limits of the A/D converter will be converted as either the maximum or minimum voltage, so information is lost.

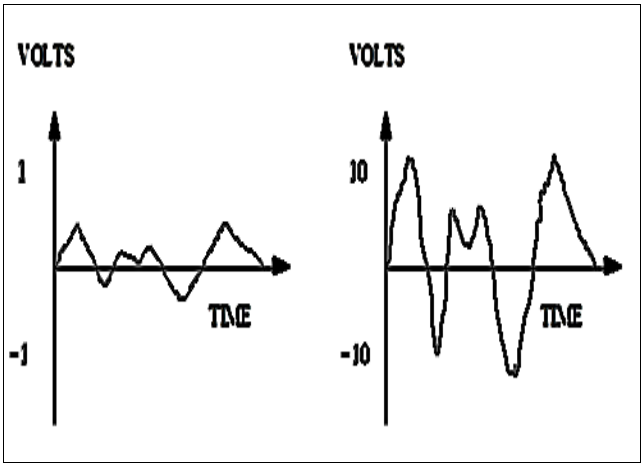

Fig 3.2: Real Time Multi-Analyzer On-Line data acquisitionsynopsis

- **Anti-aliasing:** It is the appearance of fraudulent information that occurs because of the lagging of sampling process with respect to the input rate. To avoid this anti-aliasing filters are used. These are nothing but the low pass filters that stops any frequency greater than half the sampling frequency passing through it, approximately.

- **Digitization:** In this step, the analog signals are converted into digital information in an A/D (Analog/ Digital) converter. This signal must be sampled (chopped) and quantified.

a. Sampling: In order to convert an analog signal into a digital one, it must first be sampled. These results are in natural sample values, which remain, continuous in amplitude but discrete in time.

Figure 3.3 shows both pre and post sampling of a sinusoidal wave. The sample values are exactly equal to the original signal value at the sampling instant. The amplitude of the analog signal is measured at discrete points in time using a sample and hold circuit. The process of sampling leads to the frequency spectra of the base-band signal being reproduced around the sampling frequency.

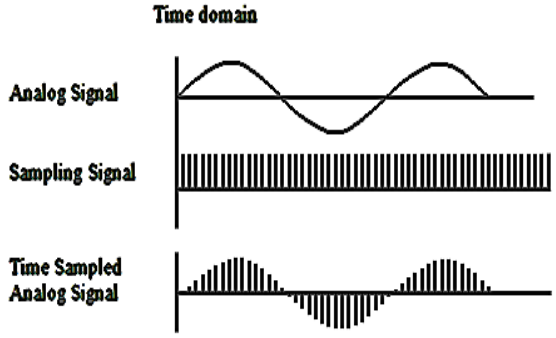

Fig 3.3: Sampling of sinusoidal wave

The choice of sampling frequency is very important. According to the sampling theorem, to be able to reconstruct a sampled signal accurately, the sampling frequency must be greater than twice the highest frequency contained in the signal to be sampled. This is called "Nyquist Frequency"
Nyquist Frequency fn = 2* fc
Where fc is the highest frequency present within the signal.
To compensate for roll-off of the anti-aliasing filter-sampling frequency must be at least
2.56 times the highest frequency.

b. Quantification: Most of the spectrum analysers have 12-bit A/D converter. This means there are 12 binary values used to represent amplitude. The A/D converter takes the continuous input data from the output of the anti-aliasing filter, approximates its characteristics, and stores as a binary number.

c. Buffer memory: The 12 bit data from A/D converter go into a memory called a buffer memory. The buffer memory holds 1024 digitized time points in bin for later decomposition to 400 frequency points. If one plotted the amplitude value in each successive bin over a time increment of 1/1024 of the time required to fill the buffer, the result would look like a display of the time waveform. When all 1024 bins are full, a photograph is taken, freezing the information for use in the FFT calculation.

d. Weighing: Suppose that a waveform if fed into the buffer memory such that two succeeding photographs would show a discontinuity. The analyzer will assume this discontinuity as an impulse in actual data and will present the user with the FFT of a periodic plus impulse spectra yielding gross error. To protect against such false discontinuities, a spectrum analyzer multiplies the time buffer by various windows.

In one type of window, the information at the end of each window is multiplied by zero. Therefore, all the adjacent time windows will have the same value i.e. zero at bin1 and 1024, which will avoid the wasting of analysers time in dealing with fictitious impulses. The waiting windows may cause slight error in amplitude values but the error is insignificant compared to the large error that could result from not doing the weighting at all. One problem with weighting windows is that, it seriously damages the data at the ends of the windows.

e. FFT: Each time when the buffer has filled with 1024 time data points, a FFT calculation is done. The resolution of each of each 400 filters is given by

β = Analysis range/ 400

The amplitude in each bin will be the RMS value calculated by the FFT. The phase calculation will be useful only for two channels or synchronous time averaging modes of operation.

f. Averaging: The averaging of the signal enhances the signal to noise ratio of the data. Several types of averaging can be done by spectrum analyser.

g. After the averaging: The average spectral values calculated can be converted into analog form using D/A converter to display on analog devices. The digitized information is available in certain formats to feed into digital devices.

IV. DEFECTS IN THE BEARINGS

Two types of known defects are introduced in two different bearings of same specification (6210*) as shown in figure 4.1 (a) and figure 4.1 (b). The defects induced are:
a) Outer race: Axial groove on inner surface of the outer race
b) Inner race: Axial groove on outer surface of the inner race

The grooves are of width 1mm, depth 1.5mm and length equal to thickness of the bearing. The defects are induced using the Electric Discharge Machining (EDM).

Figure 4.1(a): Outer race defect: Axial groove on inner surface of the outer race

Figure 4.1(b): Inner race defect: Axial groove on outer surface of the inner race

V. EXPERIMENTAL SET UP

The Experimental set up consists of shaft mounted on two bearings driven by 0.25 HP variable speed D. C. motor. The whole assembly is mounted on the rigid and heavy platform as shown in Figure 5.1, 5.2,5.3 and 5.4. The provision is made to mount an accelerometer on the bearing housings so that the bearings can be checked in the single setup.

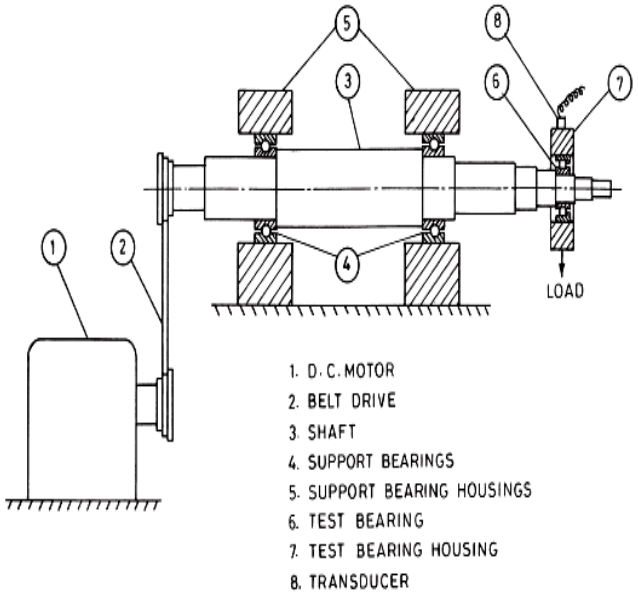

Fig 5.1: Schematic layout of the experimental setup

Fig 5.2: Experimental setup

Fig 5.3: Experimental Set-up and FFT Analyser

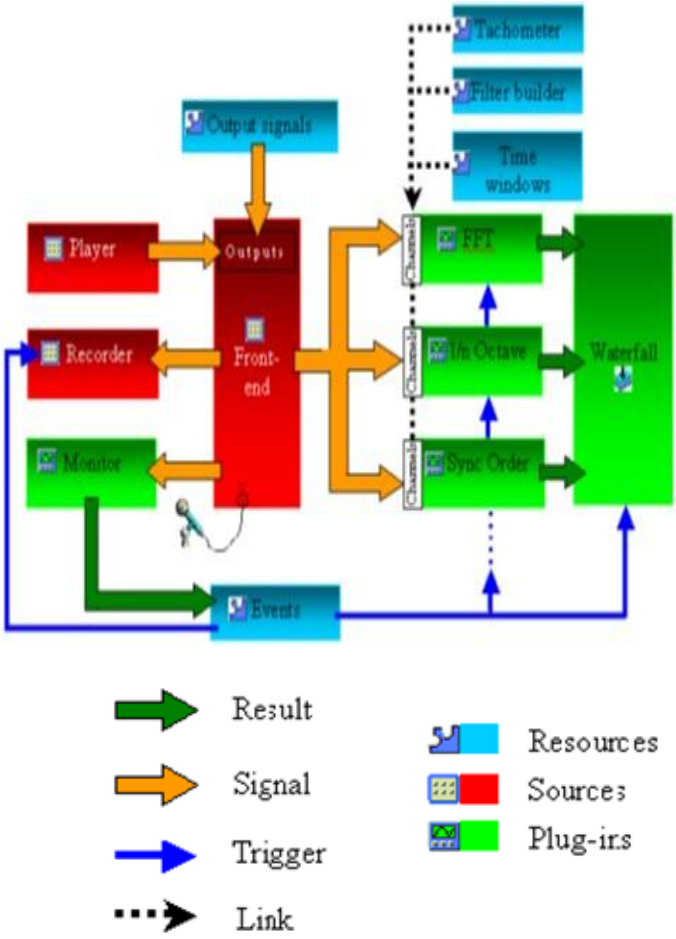

Fig5.4: Real Time Multi-Analyser On-Line data acquisitionsynopsis

5.1 EXPERIMENTAL METHODOLOGY

The following methodology is followed at the time of taking the readings,Fix the standard non-defective bearing to one of the bearing housing of the set up.

1. Mount the accelerometer over the bearing housing with the help of the stud(to collect the vibrations of the bearing)
2. Connect the accelerometer to the Real Time FFT Analyser with the help of low noise cable.
3. Start the motor and set it to the required RPM.
4. Feed the sampling frequency, sampling range and number of averages to the FFT analyser. The FFT will display the time domain and frequency domain graphs after the given number of averages.
5. The load on the shaft is varied and data are collected again for these loading conditions of the shaft at different speeds. These values will be used for comparing the data obtained from the defective bearings.
6. The same procedure is repeated with the bearings induced with known defects, and data is collected for these bearing at different speeds and different loadings.
7. Using the data obtained from the Real Time FFT Analyser, this data will be trained into the Artificial Neural Networks for analysis.

By observing the graphs given by FFT, the defects in the bearing can be identified. The data points of the graph are stored in the system. Using Excel or Mat lab graphs are reproduced and further analysis can be done.

VI. RESULTS

6.1 RESULT SHEET

The amplitude of the vibration signals are sensed and recorded using the FFT Analyser set-up. The analyser transforms the time domain signals to the frequency domain. The results are obtained as plot (both time domain and frequency domain) and the data of these plots are stored numerically.

For analysis purpose, only the amplitudes at the theoretically calculated defect frequencies are considered. Table 6.1 and6.2 gives the results in condensed form.

*H- Horizontal, *V-Vertical

a) Acceleration	*b) Frequency components*	**RPM-2500, Defect Frequency 170.5Hz**			
		Load in kg , Acceleration (mm/sec^2)			
		10	**20**	**30**	**40**
INPUT1	**1XH**	17.2900	10.8300	7.7000	7.0800
	2XH	16.4600	9.4700	7.6000	7.2100
	3XH	15.5300	10.0100	7.4300	6.7200
	4XH	13.9500	8.6000	3.9860	4.7560
	5XH	13.5400	8.4500	6.8500	6.4400
INPUT2	**1XV**	8.0000	2.6730	1.3480	1.1400
	2XV	8.2600	2.8640	1.4690	1.2840
	3XV	9.3700	2.7300	1.5170	1.3720
	4XV	7.7100	2.9600	1.7550	1.6850
	5XV	7.2400	3.8130	3.8830	3.4420

Table 6.1: Amplitude at defect frequency, BPFO

c) Acceleration	*d) Frequency components*	**RPM-2500, Defect Frequency 246.15Hz**			
		Load in kg , Acceleration (mm/sec^2)			
		10	**20**	**30**	**40**
INPUT1	**1XH**	17.35	14.03	13.82	9.93
	2XH	14.01	11.33	10.97	8.31
	3XH	11.47	9.62	10.63	8.04
	4XH	8.89	8.18	7.61	5.82
INPUT2	**1XV**	15.51	14.73	14.93	14.02
	2XV	12.69	11.95	11.71	11.32
	3XV	10.44	10.23	11.16	10.63
	4XV	10.24	9.63	10.63	10.7

Table 6.2: Amplitude at defect frequency, BPFI

6.2 RESULTS AND DISCUSSION

The results are based on the change in amplitude at defect frequencies calculated for bearings from the equations derived. These frequencies and corresponding amplitudes are measured from the spectrum obtained in FFT analyser.

Vibration spectrum obtained for bearings without defect and with various defects is given for load condition, and at 2500 RPM. (Figure 6.1 to 6.9).

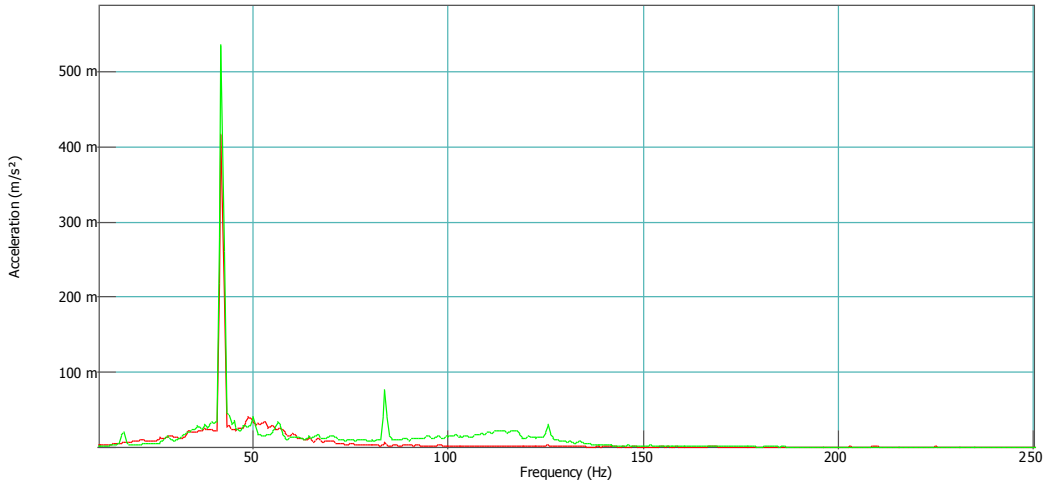

Fig 6.1: Frequency spectrum for bearing without defect, no load, at 2500RPM

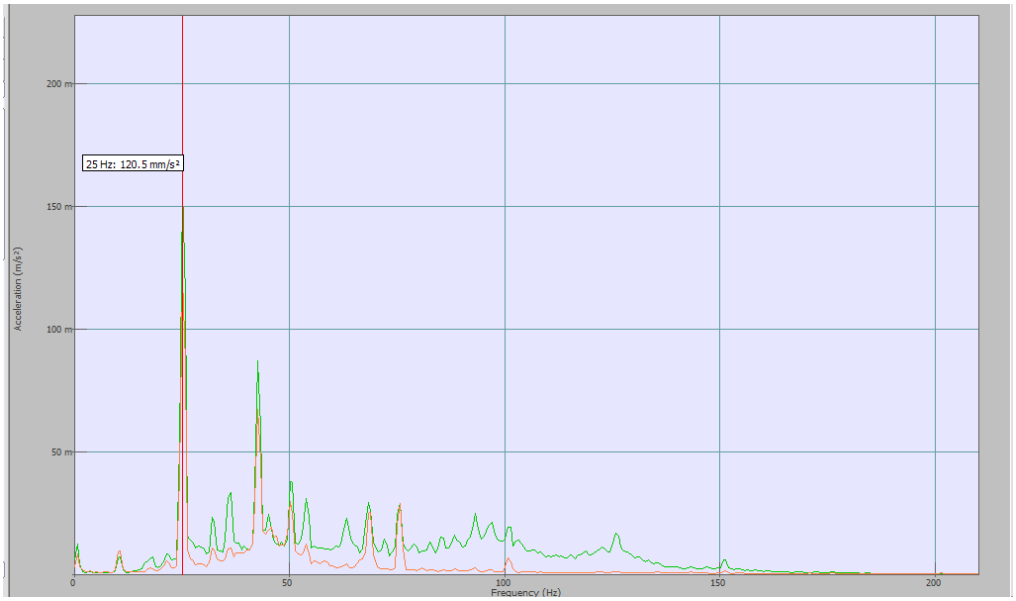

Fig 6.2: Frequency spectrum for bearing without defect, no load, at 2500RPM

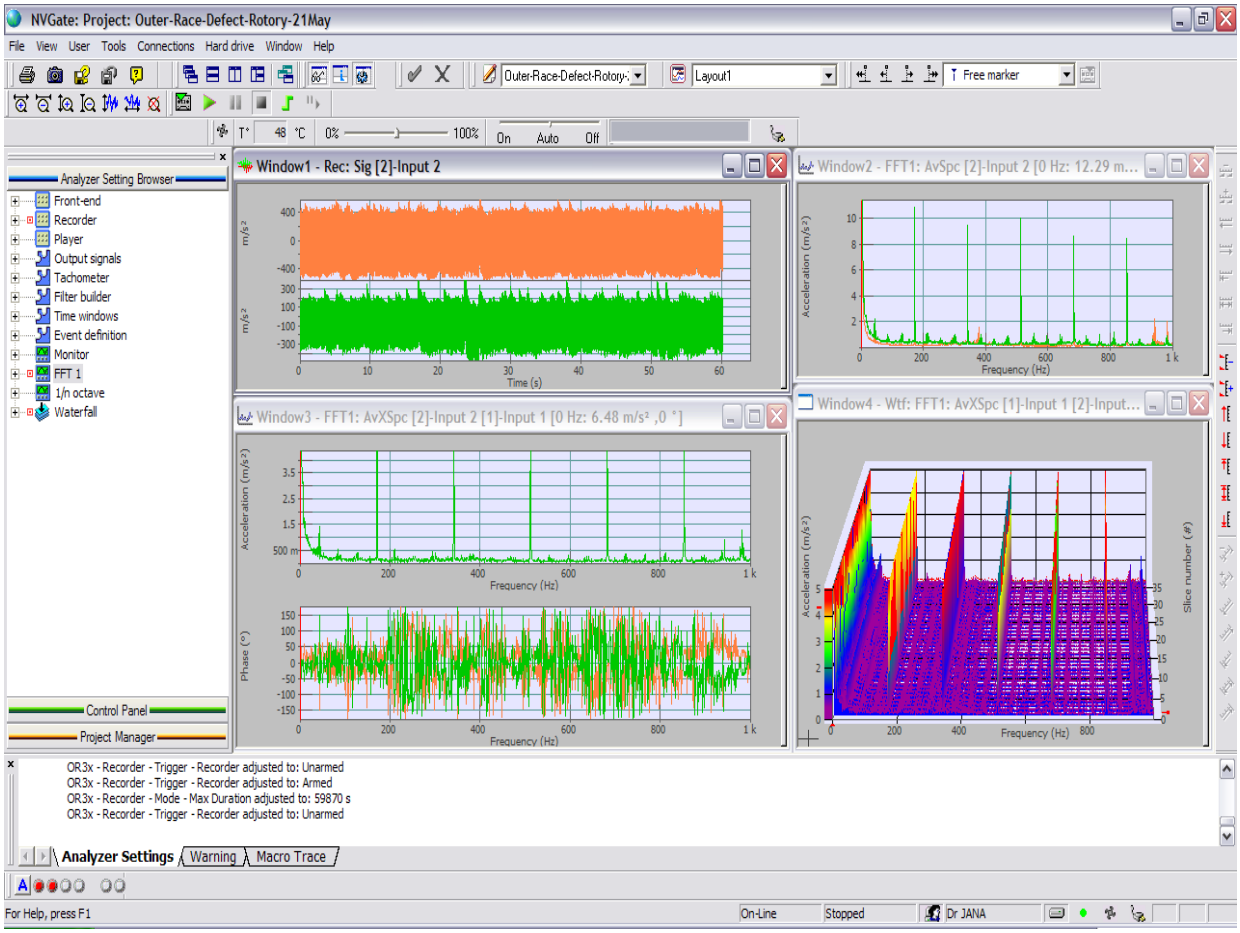

Fig 6.3: Frequency spectrum for bearing with outer race defect, 40Kg load, at 2500RPM

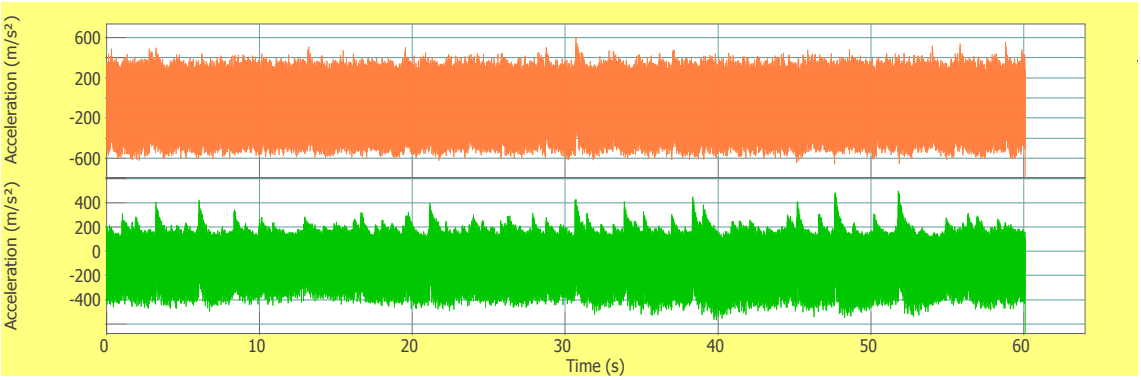

Fig 6.4: Time domain signal of outer race defect, load 40Kg, at 2500 RPM

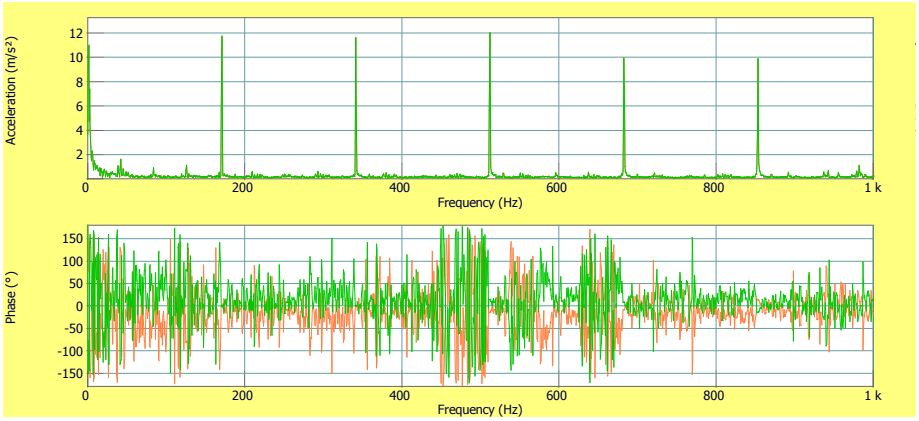

Fig 6.5: Frequency average spectrum of outer race defect, load 40Kg, at 2500 RPM

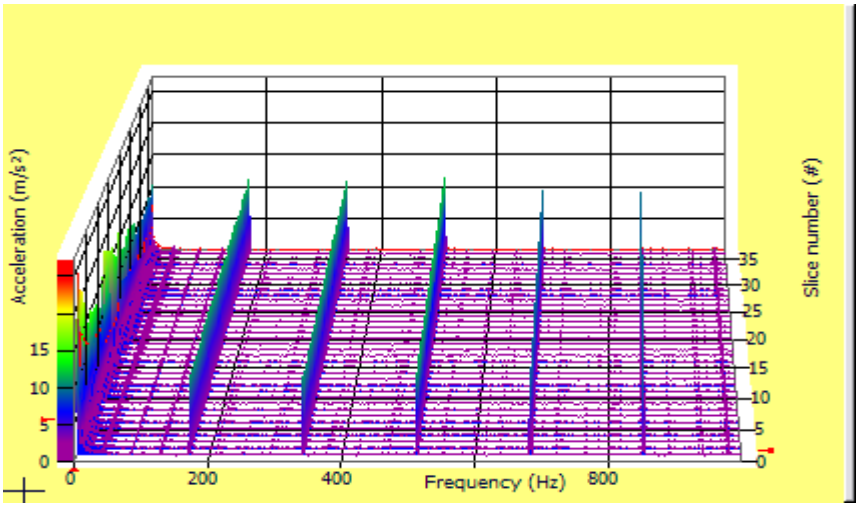

Fig 6.6: Outer Race defect waterfall diagram, load 40Kg, at 2500 RPM

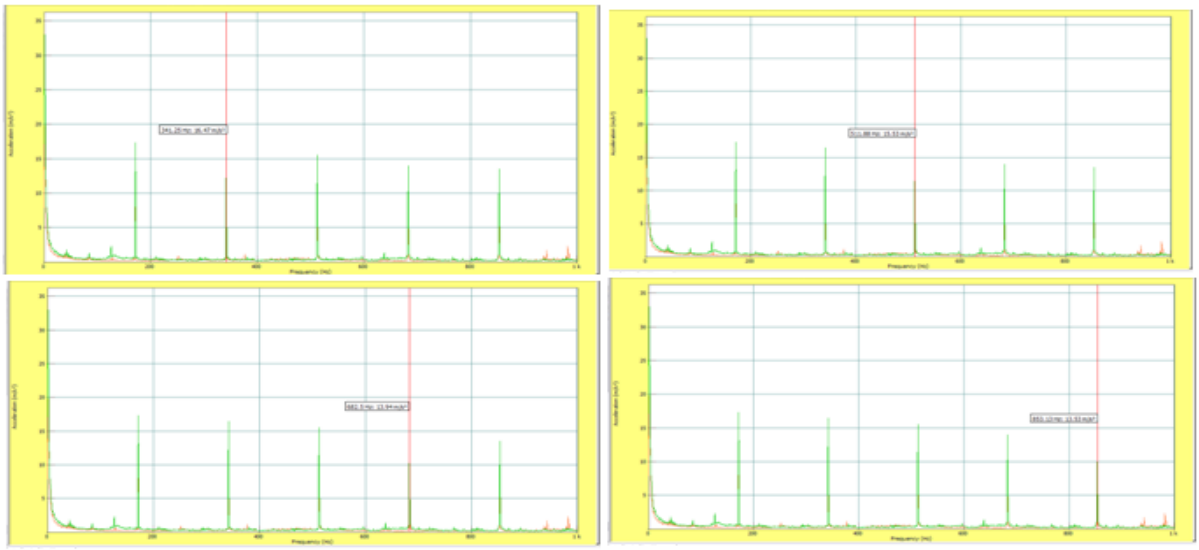

Fig6.7: Frequency spectrum of Outer Race defect, load 40Kg, at 2500 RPM

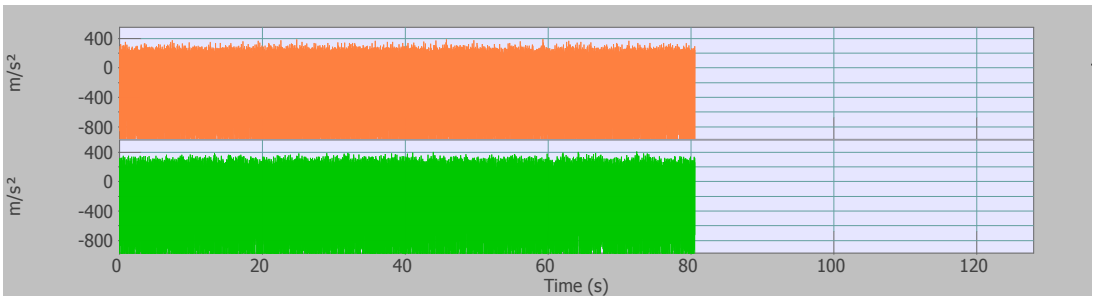

Fig 6.8: Time domain Inner Race defect, load 40Kg, at 2500 RPM

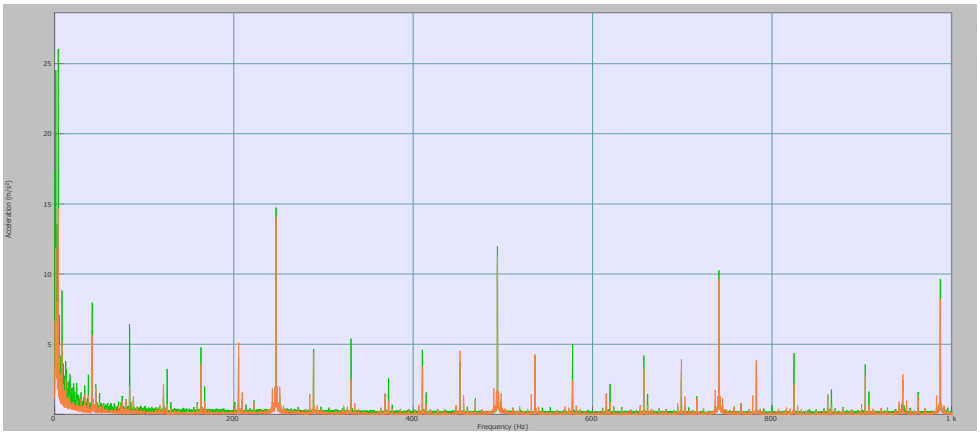

Fig 6.9: Frequency Spectrum of Inner Race defect, load 40Kg, at 2500 RPM

VII. TRAINING AND TESTING DATA

7.1 NETWORK TRAINING AND TESTING OF OUTER RACE BEARING DATA

The training and test data, during the present study were generated on a rotor test rig Fig.7.1 (a) and (b). The table 7.1 shows the training data and test data of acceleration (mm/s2)for various outer races bearing data in horizontal and vertical directions. The training of the neural network involves adjusting the weights such that the error between network output and the desired output is a minimum. The error function is usually expressed as the difference between the desired network response and its real output. In general, the error function is a multi-variable vector and can be optimized by using non-linear programming techniques such as gradient decent back propagation, and Levenberg-Marquardt algorithms. In this case the ratios of convergence

speeds of this method are 1, 10 and 100 respectively. The Levenberg-Marquardt algorithm has the best convergence speeds for small and medium size networks.

The values of frequency components in the horizontal and vertical directions for outer races bearing load ranging from 10 to 40 kg and speed is 2500 RPM. Three sets of data are trained by using Mat Lab Neural Network Tool Box. Network is said to be trained when the epochs are maximum, learning rate μ is maximum and error is minimum. The training has been carried out using of error goals from 0.01 to 0.0001, with different number of neurons. Since there is no specific method to decide about the exact number of neurons in the hidden layer, an empirical geometrical pyramid rule will be discussed [3]. Number of hidden neurons = √mn, Where m = Number of output neurons, n = Number of input neurons. In this case the value of m =3, and n = 12. The number of hidden neurons according to empirical rule will be 6. The network was trained using 6 neurons with error goal combinations of 0, 0001. The testing was carried out using the test set given in the last column of table 7.2. From table 7.2, with error goal of 0.0001 and 8 neurons it is seen that in training number 2, the epochs and (μ) remaining constant the sum squared error became the least leading to good generalization. Table 7.3 shows the values of frequency components in the horizontal and vertical directions for outer race bearing ranging from 10 to 40kg. Three sets of data are trained by using Mat Lab Neural Network Tool Box. Network is said to be trained when the epochs are maximum, learning rate μ is maximum and error is minimum. After successful training, the Network is tested for simulation with a separate set of untrained data. It is observed that the Neural Network is able to detect the corresponding outer race bearing load of 39.970 kg for epochs of 4 and an error of 33.3333/0.001for an error goal 1e-010.

The experimental value of outer race bearing is 40 kg. The Network has identified the value of unbalance to an accuracy of 99.93 %. This is in close correlation with the experimental values.

*H- Horizontal, *V-Vertical

Table 7.1: Network training data and test data of acceleration for outer race bearing load ranging from 10 kg to 40 kg and a bearing speed of 2500 RPM.

e) Frequency components	**Outer race Bearing Load in kg**			**Test data (mm/s^2)**
	Training data (mm/sec^2)			
	10	**20**	**30**	**40**
1XH	17.2900	10.8300	7.7000	7.0800
2XH	16.4600	9.4700	7.6000	7.2100
3XH	15.5300	10.0100	7.4300	6.7200
4XH	13.9500	8.6000	3.9860	4.7560
5XH	13.5400	8.4500	6.8500	6.4400
1XV	8.0000	2.6730	1.3480	1.1400
2XV	8.2600	2.8640	1.4690	1.2840
3XV	9.3700	2.7300	1.5170	1.3720
4XV	7.7100	2.9600	1.7550	1.6850
5XV	7.2400	3.8130	3.8830	3.4420

Table 7.2: Quantification of Outer race bearing load, error goal 0.0001 and hidden neurons 6

erial no.	**Experimental values of outer race bearing load (kg)**	**Epochs**	**MSE**	**ANN Quantification values**	**Percentage**
1	**10**	**4**	**33.3333/0.001**	**9.9840**	**99.84**
2	**20**	**4**	**3.12067e+006**	**19.924**	**99.62**
3	**30**	**4**	**77.7778/0.001**	**29.624**	**98.74**
4	**40**	**4**	**33.3333/0.001**	**39.970**	**99.93**

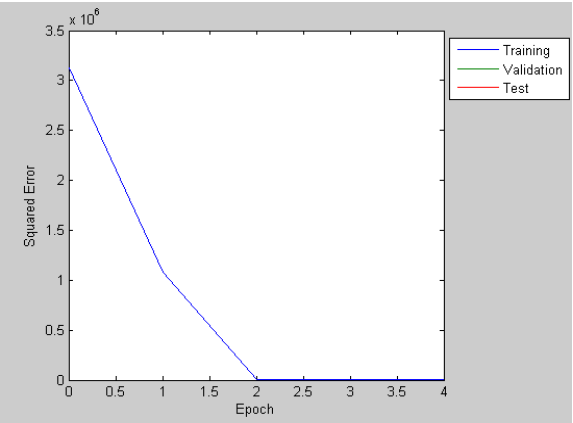

Figure 7.1 (a): Epoch versus Training bluegoal black, (b): Epoch versus squared error

7.2 NETWORK TRAINING AND TESTING OF INNER RACE BEARING DATA

The training and test data, during the present study were generated on a rotor test rig Fig.7.2 (a) and (b). The table 7.4 shows the training data and test data of acceleration (mm/s^2)for various inner races bearing data in the horizontal and vertical directions. The training of the neural network involves adjusting the weights such that the error between network output and the desired output is a minimum. The error function is usually expressed as the difference between the desired network response and its real output. In general, the error function is a multi variable vector and can be optimized by using non-linear programming techniques such as gradient decent back propagation, and Levenberg-Marquardt algorithms. In this case the ratios of convergence speeds of this method are 1, 10 and 100 respectively. The Levenberg-Marquardt algorithm has the best convergence speeds for small and medium size networks.

The values of frequency components in the horizontal and vertical directions for inner races bearing load ranging from 10 to 40 kg and speed is 2500 RPM. Three sets of data are trained by using Mat Lab Neural Network Tool Box. Network is said to be trained when the epochs are maximum, learning rate μ is maximum and error is minimum. The training has been carried out using of error goals from 0.01 to 0.0001, with different number of neurons. Since there is no specific method to decide about the exact number of neurons in the hidden layer, an empirical geometrical pyramid rule will be discussed [3]. Number of hidden neurons = √mn, Where m = Number of output neurons, n = Number of input neurons. In this case the value of m =3, and n = 12. The number of hidden neurons according to empirical rule will be 6. The network was trained using 6 neurons with error goal combinations of 0, 0001. The testing was carried out using the test set given in the last column of table 7.4. From table 7.4, with error goal of 0.0001 and 8 neurons it is seen that in training number 2, the epochs and (μ) remaining constant the sum squared error became the least leading to good generalization. Table 8.4 shows the values of frequency components in the horizontal and vertical directions for inner race bearing ranging from 10 to 40kg. Three sets of data are trained by using Mat Lab Neural Network Tool Box. Network is said to be trained when the epochs are maximum, learning rate μ is maximum and error is minimum. After successful training, the Network is tested for simulation with a separate set of untrained data. It is observed that the Neural Network is able to detect the corresponding inner race bearing load of 39.922 kg for epochs of 6 and an error of 33.3333/0.001for an error goal 1e-010.
The experimental value of inner race bearing is 40 kg. The Network has identified the value of unbalance to an accuracy of 99.922 %. This is in close correlation with the experimental values.
*H- Horizontal, *V-Vertical

Table 7.3: Network training data and test data of acceleration for inner race bearing load ranging from 10 kg to 40 kg and a bearing speed of 2500 RPM.

f) Frequency components	**Inner race Bearing Load in kg**			**Test data (mm/s^2)**
	Training data (mm/sec^2)			
	10	**20**	**30**	**40**
1XH	17.35	14.03	13.82	9.93
2XH	14.01	11.33	10.97	8.31
3XH	11.47	9.62	10.63	8.04
4XH	8.89	8.18	7.61	5.82
1XV	15.51	14.73	14.93	14.02
2XV	12.69	11.95	11.71	11.32
3XV	10.44	10.23	11.16	10.63
4XV	10.24	9.63	10.63	10.7

g) Table 7.4: Quantification of inner race bearing load, error goal 0.0001 and hidden neurons 6

Figure 7.2(a): Epoch versus Training bluegoal black, (b): Epoch versus squared error

Serial no.	Experimental values of inner race bearing load (kg)	Epochs	MSE	ANN Quantification values	Percentage
1	**10**	**7**	**33.3333/0.001**	**9.8980**	**98.98**
2	**20**	**4**	**77.7778/0.001**	**19.924**	**99.62**
3	**30**	**7**	**77.7778/0.001**	**29.9680**	**99.89**
4	**40**	**6**	**33.3333/0.001**	**39.9220**	**99.80**

VIII. CONCLUSION

From the analysis of the various plots obtained based on the experimental and analysis results the following conclusions can be made:

- It is observed that for the same defect frequency, the vibration amplitude for the defective bearing is much higher than that for non-defective bearing. Thus, we can conclude that the rise in the vibration level is an indication of presence of defect.
- It is also observed that the amplitude of the vibration signal shows a descending trend with the increase in the load at all the defect frequency. Thus, it is concluded that with the increase in the load, the vibration level decreases.
- The corresponding amplitude at the respective defect frequencies also shows an upward trend for the bearing without any defect. However, this rise in the vibration level is negligible when compared with that in the bearings with defects.
- It is observed that the Neural Network is able to detect the corresponding Value of bearing defect.
- The experimental value of inner race bearing. The Network has identified the value of unbalance to an accuracy of 99.922 %. This is in close correlation with the experimental values.
- The experimental value of outer race bearing. The Network has identified the value of unbalance to an accuracy of 99.93 %. This is in close correlation with the experimental values.
- This neural network has an edge over conventional monitoring method that can classify the condition of machine components even in the absence of explicit input–output relationships. Besides, the network can classify well even in the case of noisy or incomplete information obtained from the signals being monitored.

REFERENCES

[1] H. K. Srinivas, K. S. Srinivasan, K. N. Umesh.,Application of Artificial Neural Network andWavelet Transform for Vibration Analysis ofCombined Faults of Unbalances and Shaft Bow,Adv. Theor. Appl. Mech., Vol. 3, 2010, no. 4, 159 – 176.

[2] Dutt, J. K. and Nakra, B. C., Stability of Rotor System with Viscoelastic Support, Journal of Sound and Vibration, 153 (1), (1993), 89 –96.

[3] Genta, G. and De Bona, F. Unbalance Response of Rotors; A Modal Approach with Some Extensions to Damped natural Systems , Journal of Sound and Vibration, 140 (1), (1990), 129 –153.

[4] S. Edwards, A. W. Lees, and M. I. Friswell. Fault Diagnosis of Rotating Machinery, The Shock and Vibration Digest, 30 (1), (1998), 4-13.

[5] Gasch, R., A survey of the dynamic Behavior of a Simple Rotating Shaft with a Transverse Crack , Journal of Sound and Vibration, 160 (2), (1993), 313-332.

[6] Meng, G. and Hahn, E. J. , Dynamic Response of Cracked Rotor With some Comments on Crack Detection , Journal of Eng. Gas Turbines and Power, 119 (2), (1997), 447 –455.

[7] Isermann, R., Supervision, Fault detection and Fault-Diagnosis methods, Control Eng. Practice, 5(5), (1997), 639 – 652,

[8] A.W. Lees and M. I. Friswell, The Evaluation of Rotor Imbalance in Flexibly Mounted Machines, Journal of Sound and Vibration, 208(5), (1997), 671-683.

[9] D. L. Hall, R. J. Hansen and D. C. Lang , The Negative Information Problem in Mechanical Diagnostics , Journal of Eng. for Gas Turbines and Power, 119,(1997) , 370-377.

[10] K. S. Srinivasa, Fault Diagnosis in Rotating Machines Using Vibration Monitoring and Artificial Neural Networks, Ph. D Thesis, ITMMEC, Indian Institute of Technology Delhi, (2003).

[11] K. S. Srinivasan and Umesh K. N., Study of effects of Misalignment on vibration Signatures of Rotating Machinery, National Conf. README-05, PACE, Mangalore,(2005).

[12] A. C. McCormick and A. K. Nandi, A Comparison of Artificial Neural networks and other statistical methods for rotating machine condition classification, IEE, savoy London, (1996), 2(1)-2(6).

[13] A. C. McCormick and A. K. Nandi, Classification of the rotating machine condition using artificial neural networks, Proceedings Instrumentation Mechanical Engineers, 211, Part-C, (1997) , 439-450.

[14] NalinakshS.Vyas and D. Sathishkumar, Artificial Neural Network Design for Fault identification in Rotor-Bearing System, 36, Mechanism and Machine Theory, (2001), 157-175.

[15] M. Kalkat and S.Yildirim and I. Uzmay , Rotor Dynamics Analysis of Rotating Machine Systems using Artificial Neural Networks, International Journal of Rotating Machinery, 9, (2003), 255-262.

[16] Nahvi and M. Esfahanian, Fault identification in rotating machine condition using artificial neural networks, Proceedings Instrumentation Mechanical Engineering Science, 219, (2004), 141-158.

[17] .JeongSooRyu, Doo Byang Yoon and Jong sup wu, Development of a HANARO Vibration Monitoring System for Rotating Machinery, Proceedings of the Internal Symposium on Research Reactor and Neutron Science, (2005).

[18] T. S. W. Chow and L. T. Jaw, city polytechnic of Hong Kong, Rotating machines Fault identification using BackPropagation Artificial Neural Network, 405-412.

[19] G. G. Yen and Kuo-Chung Lin, Wavelet Packet Feature Extraction for Vibration Monitoring, IEEE Transactions on Industrial Electronics, 47, no 3, (2000), 650-666.

[20] D. Boras, M. Castila, N. Moreno and J. C. Montano, Wavelet and Neural Structure; A New Tool for Diagnostic of Power System Disturbances, IEEE, Transactions on Industry Applications, 30, no 1 (2001), 184-190.

[21] Xie FL, Flowers G. T., Feng L. and Lawrence C., Steady State Dynamic Behavior of Flexible Rotor with Auxiliary Support from Clearance Bearing, Journal of Vibration and Acoustics, Vol. 121/79, 1999, 78-83.

[22] D. Muller, A.G. Sheard., S. Mozumdar., and E. Lohann., Capacitive measurement of compressor and turbine blade tip to casing running clearance, Journal of engineering for gas turbines and power , Vol. 119, Oct 1997, 877-884.

[23] Sang-Kyu Choi, and Sherif T. Noah., Mode locking and chaos in a Jeffcott rotor with bearing clearances, Journal of applied mechanics, vol. 61, Mar. 1994, 131-138.,513461–3468, 2006